

Structural and Electrical Properties of PbTiO_3 Thin Films Grown on Silicon Substrates

D. Remiens, B. Jaber, P. Tronc & B. Thierry

CRITT Céramiques Fines, Laboratoire des Matériaux Avancés Céramiques, Université de Valenciennes et du Hainaut-Cambrésis, Z.I. Champ de l'Abbesse, 59600 Maubeuge, France

(Received 18 November 1994; revised version received 30 June 1995; accepted 14 July 1995)

Abstract

Thin films of ceramic materials take an important place in microelectronics and in microtechnologies. They present many properties which can be used for the realization of new devices and sensors. We present the growth of PbTiO_3 thin films on silicon and platinized silicon substrates by RF magnetron sputtering. The electrode deposition and thicknesses were optimized to produce metallization without the defects which are frequently observed with Pt electrodes. The influence of the bottom electrodes on the film properties in terms of structure and microstructure was analysed. The PbTiO_3 crystallization was optimized for the two types of substrates: Si/SiO_2 and $\text{Si}/\text{SiO}_2/\text{Ti}/\text{Pt}$. The electrical properties of the films and in particular the ferroelectricity were evaluated.

1 Introduction

Recently, interest in ferroelectric thin films has grown rapidly with active studies directed towards exploring several ferroelectric compositions, while involving a variety of deposition techniques. The techniques usually used for fabricating ferroelectric thin films have included sol-gel processing,¹ metallo-organic chemical vapour deposition (MOCVD),² laser ablation³ and radio-frequency (RF) magnetron sputtering.⁴ Sputtering is very well adapted to grow ferroelectric thin films at low temperatures and for optical applications.⁶ The growth of ferroelectric thin films on silicon substrates offers several advantages for integrated circuit and miniaturized devices. The applications are very important: piezoelectric and pyroelectric sensors, electro-optic devices and non-volatile memories. For many applications the silicon substrate must be metallized: a Ti/Pt electrode is usually used mainly because of its superior barrier effect against chemical reactions between the film and the Si substrate.

We report on the growth of PbTiO_3 thin films, deposited at room temperature, from an oxide target by RF magnetron sputtering. The films were deposited onto different substrates: oxidized (100) silicon (Si) wafers and oxidized (100) Si coated with Ti–Pt electrodes. A subsequent annealing treatment was performed to crystallize the film. The electrodes have an important influence on the film properties and so we have optimized the metallization growth conditions and annealing treatment. We have studied the influence of the electrodes on the PbTiO_3 film qualities and, in particular, on the structures and the microstructures. Electrical properties were evaluated by measuring the ferroelectric behaviour.

2 Experimental Procedures

An RF magnetron sputtering system, described previously,⁷ was used to prepare PbTiO_3 thin films. The sputtering target was a mixture of PbO and TiO_2 powders; they were obtained by uniaxially cold pressing. The targets composition are $x\text{PbO} + y\text{TiO}_2$ where x and y represent the mole fraction of PbO and TiO_2 , respectively. The sputtering conditions used in this experiment are summarized in Table 1; depositions were performed at room temperature. For targets $0.54\text{ PbO} + \text{TiO}_2$, the films are nearly stoichiometric ($\text{Pb}/\text{Ti} = 1.15$). The lead excess is evaporated during the post-annealing treatment to obtain stoichiometric films. The substrate temperature increased during sputtering (60°C), induced by the particle bombardment (electrons, ions, etc.).

We have limited the RF power to 10 W; for higher power, microcracks appear at the single composite oxide surface target and, more precisely, in the erosion area (magnetron system) after a few hours of sputtering. The target contains much porosity (the target fabrication is described previously⁸), which limits evacuation of

Table 1. Sputtering conditions for preparation of PbTiO₃ films

RF power	10 W
Target diameter	25 mm
Target composition	0.54 PbO + TiO ₂
Interelectrode distance	35 mm
Gas pressure	100 mT
Sputtering gas	Ar
Substrate temperature	Ambient–60°C

the energy loss in the target during sputtering and so induces thermal stress.

These growth conditions were selected in order to have a relatively important deposition rate (for oxides), which is of the order of 20 Å min⁻¹ on Si/SiO₂ substrates. The substrate preparation before the growth is crucial to obtain PbTiO₃ film of good crystalline quality and adherence. We have used a procedure well known in semiconductor technology⁹ for the preparation of the Si/SiO₂. The Si/SiO₂/Ti/Pt substrates were only degreased and dried. The film thicknesses were measured by profilometry. Then, after photolithography the films were chemically etched to make a step between the film and the substrate. The deposition of Ti/Pt metallization is an important parameter, directly related to the ferroelectric thin film properties. We have studied the growth and annealing conditions of the Ti/Pt layers.

Since the films were deposited on unheated substrates they were amorphous and a post-deposition annealing was necessary to crystallize the film into the perovskite structure. We have used conventional annealing and have optimized the annealing parameters, i.e. temperature and time, for both the Si/SiO₂ and Si/SiO₂/Ti/Pt structures. The presence of the metallization affects the morphology and the crystal structure formation of the PbTiO₃ film.

3 Results and Discussion

3.1 Bottom electrode deposition and post-annealing treatment

Titanium and platinum films were deposited on (100) oriented silicon substrates, passivated with a thermally grown silicon dioxide layer of 5000 Å. The same substrates without metallization were used for the growth of PbTiO₃ films in order to study the influence of the metallization on the PbTiO₃ crystallization. The electrodes were grown by a RF magnetron sputtering technique without substrate heating. Ti/Pt metallizations were fabricated by a sequential deposition process in a single pump-down cycle without breacking the vacuum. The growth conditions were fixed in order to have a very slow growth rate: RF power is 70 W (the target diameter is 150 mm) and the

gas pressure is 20 mT. With these conditions the Pt layer is very dense and the surface morphology is smooth. The titanium layer is employed to promote adhesion. The thickness of the electrodes was varied between 100 and 500 Å for Ti and 800 and 2000 Å for Pt, and we have studied the influence of the electrode thickness on the morphology after annealing. The Pt layer presents a (111) preferred orientation just after deposition. The annealing treatment of the electrode is the same as for the PbTiO₃ films: the annealing temperature is 680°C and the annealing time is fixed to 1 h. After thermal annealing the metallized substrates were systematically observed with a scanning electron microscope (SEM). The annealing treatment induced a more pronounced (111) preferred orientation with no (200) oriented grains detectable by X-ray diffraction (XRD) analysis.

Figure 1 shows the surface morphology of Ti/Pt films after annealing; the thicknesses of Ti and Pt were 200 and 1000 Å, respectively. The platinum, originally very small-grained, has coalesced into larger grains which have holes in between them. The recrystallization of the Pt layer results in the formation of Pt droplets; the surface morphology was very rough.

A PbTiO₃ film was grown on this electrode; the morphology is a replica of the Ti/Pt layers. All test capacitors measured on these exhibit electrical shorts which are attributed to the Pt hillocks and holes formation. For a thicker Pt layer, the thickness of the Ti layer was maintained constant, the morphology is different. Figure 2 shows a scanning electron micrograph of a Ti/Pt layer after annealing; the thickness of the Pt layer is 2000 Å. The Pt layer was continuous without holes or hillocks. With such an electrode, the PbTiO₃ film presents no degradation and electrical characterizations are possible; identical results were obtained for the thicker Ti layer (500 Å).

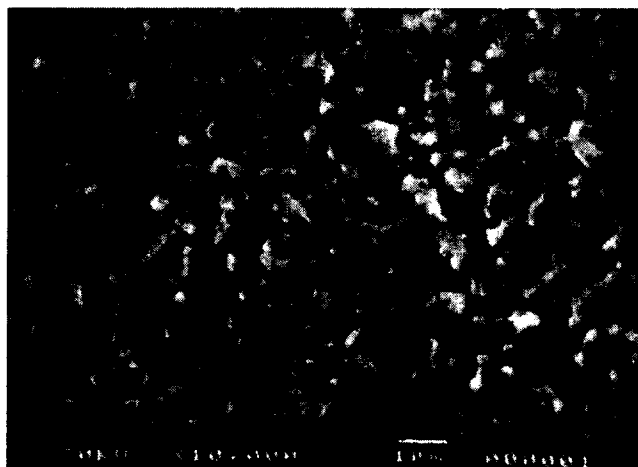


Fig. 1. SEM photograph of Ti/Pt films after annealing (Ti = 200 Å, Pt = 1000 Å).

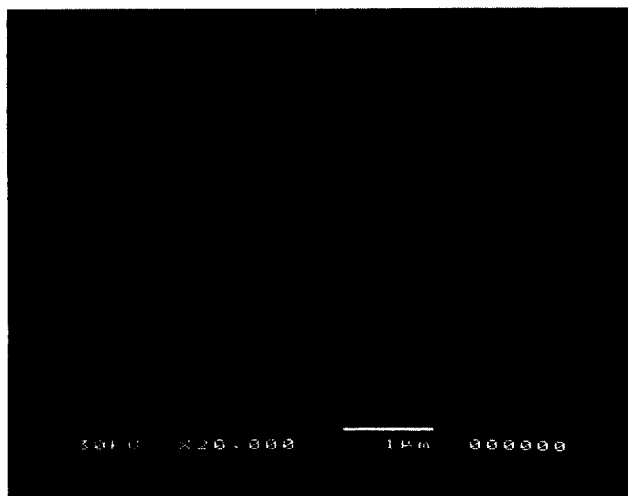


Fig. 2. SEM photograph of Ti/Pt films after annealing (Ti = 200 Å, Pt = 2000 Å).

3.2 Post-annealing treatment of PbTiO_3 on silicon and platinized silicon substrates

As we have mentioned previously, deposition of PbTiO_3 was performed at room temperature and the film is amorphous. A post-annealing treatment is necessary to crystallize the film into the perovskite phase and to remove the porosity of the film. We have optimized the conventional annealing treatment for the two types of substrates: Si/SiO₂ and Si/SiO₂/Ti/Pt (annealing at 680°C for 1 h).

Figure 3 shows the XRD pattern of the PbTiO_3 film (thickness 0.6 μm) grown on Si/SiO₂ (a) and Si/SiO₂/Ti/Pt (b) substrates; the annealing temperature is 680°C and the annealing time is 30 min. The ramp down is fixed to 5°C min⁻¹; for higher values microcracks appear on films grown on Si/SiO₂ substrates but not on Si/SiO₂/Ti/Pt. The ambient gas is air. We observed an improvement in the crystallinity of the film in the case of platinized substrates, evidenced by higher and sharper XRD peaks. The platinum layer favours the crystallization of the PbTiO_3 film. The films are preferentially (101) oriented for the two types of substrates, but the preferred orientation is more pronounced on annealing platinized substrate. Without annealing the Pt layer, the XRD pattern of the PbTiO_3 film is similar to that obtained on Si/SiO₂ substrates. The degree of orientation of Pt affects the orientation of the PbTiO_3 deposited on it. No second phases were observed to occur after annealing and the (111) Pt orientation was retained.

The annealing time influences considerably the crystallinity of the film. Figure 4 shows the XRD diffraction pattern of PbTiO_3 films grown on Si/SiO₂/Ti/Pt substrates. The annealing times are 30 min (a), 1 h (b) and 2 h (c); the annealing temperature is 680°C. When the annealing time increased, the crystallinity of the film decreased.

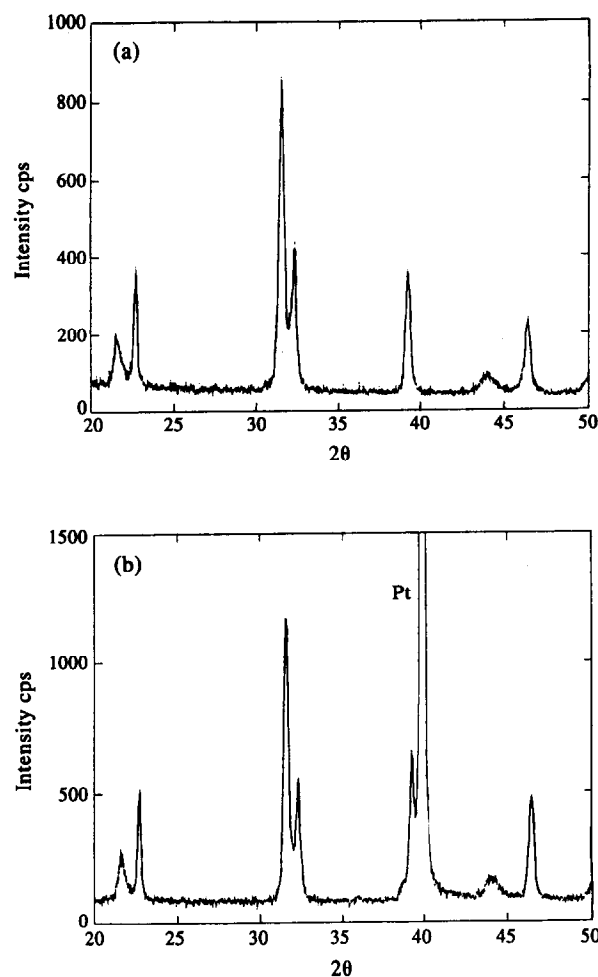


Fig. 3. (a) XRD pattern of PbTiO_3 film on Si/SiO₂ substrate (annealing temperature = 680°C, annealing time = 30 min). (b) XRD pattern of PbTiO_3 film on Si/SiO₂/Ti/Pt substrate (annealing temperature = 680°C, annealing time = 30 min).

So we can conclude that the best annealing parameters for the structure Si/SiO₂/Ti/Pt/ PbTiO_3 are 680°C for 30 min. The same study was made for Si/SiO₂ substrates; the annealing time must be fixed to 1 h to obtain a film crystallinity similar to that obtained on a platinized silicon substrate.

The annealing time controls the grain size; the grain size increased as the annealing time increased, as shown in Fig. 5 (Si/SiO₂/Ti/Pt substrates) with an annealing temperature of 680°C. For an annealing time of 30 min, the grain size is of the order of 150 nm (measured from a scanning electron micrograph) with an uniform distribution; the film has a dense morphology without porosity. A large amount of porosity appears for an annealing time of 2 h, induced by grain growth.

The same behaviour was observed for Si/SiO₂ substrates but the microstructure of the PT film appears different, having large grains with very fine grains between them. The Pt metallization seems to affect also the microstructure of the PbTiO_3 film. Further studies are in progress to confirm and to understand this behaviour.

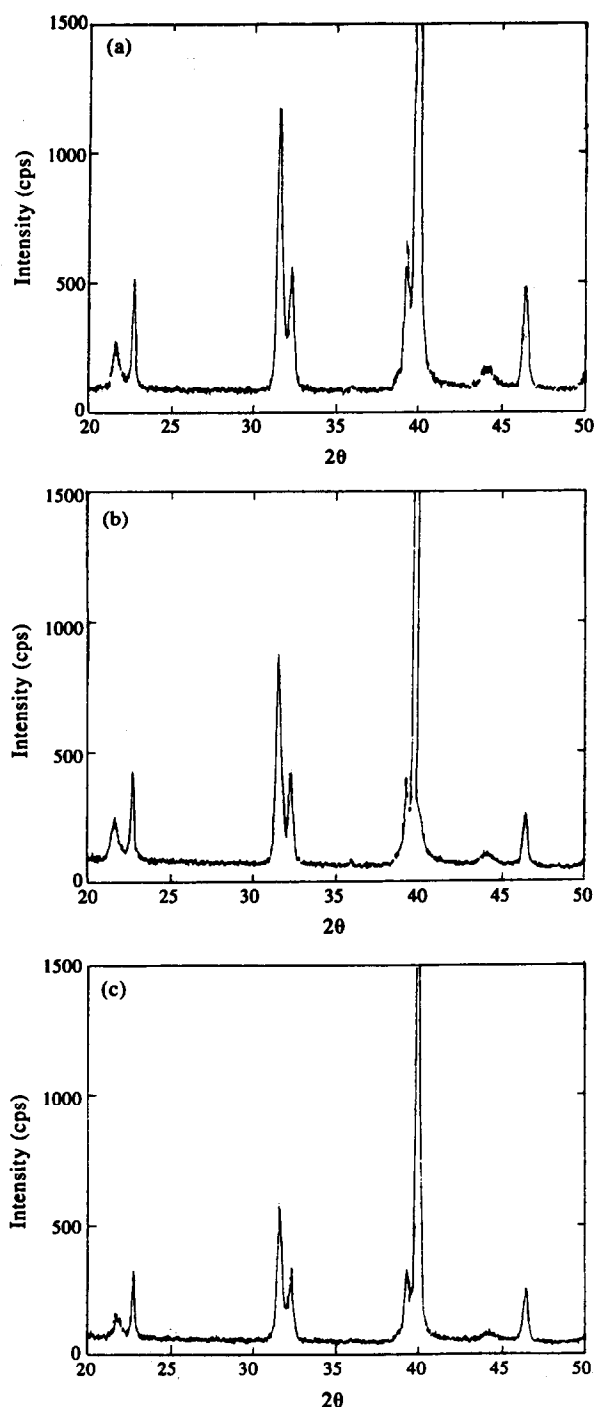


Fig. 4. XRD pattern of PbTiO_3 on $\text{Si/SiO}_2/\text{Ti/Pt}$ substrate (annealing temperature = 680°C): (a) annealing time = 30 min; (b) annealing time = 1 h; (c) annealing time = 2 h.

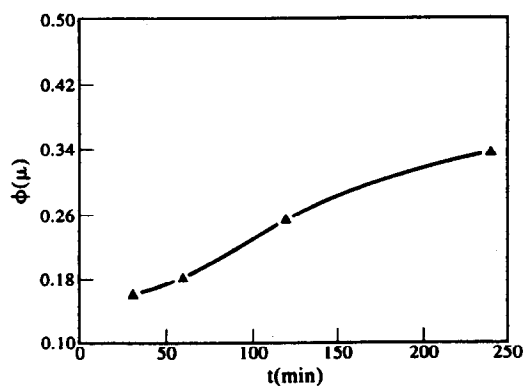


Fig. 5. Grain size as function of annealing time.

3.3 Electrical properties

Films were characterized for their electrical properties through the measurement of polarization hysteresis. Polarization reversal is generally taken as a measure of the degree of ferroelectricity. Hence, the ferroelectric nature of the films was examined by observing the hysteresis loop taken at room temperature at a frequency of 1 kHz by means of a modified Sawyer–Tower circuit.

The test capacitors were fabricated with a $\text{Si/SiO}_2/\text{Ti/Pt/PT/PT/Pt}$ structure (Fig. 6); the bottom electrode was preannealed at 680°C for 1 h before the PbTiO_3 deposition and the ferroelectric layers were annealed at 680°C for 30 min. Pt top electrodes of $100\ \mu\text{m}$ diameter were fabricated by photolithography and sputtering (lift-off process). On some test capacitors we have performed a top electrode annealing of 450°C for 1 h. All the films discussed here have a thickness of $\sim 0.9\ \mu\text{m}$.

In order to give significant results concerning hysteresis properties, it is necessary to consider all the hysteresis loops obtained at voltages between 10 and 30 V (Fig. 7). In this example, the top electrodes were not annealed. For 10 tested samples, we find an average value of the coercive field (for an applied voltage of 30 V) of $V_c^+ = 18\ \text{V}$ and $V_c^- = -12\ \text{V}$ (see Fig. 7 for notation); the remanent

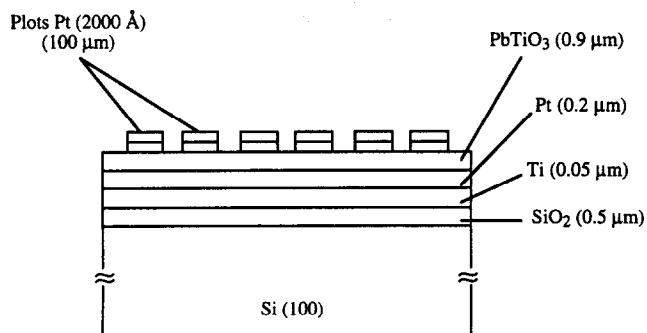


Fig. 6. Test capacitor structure.

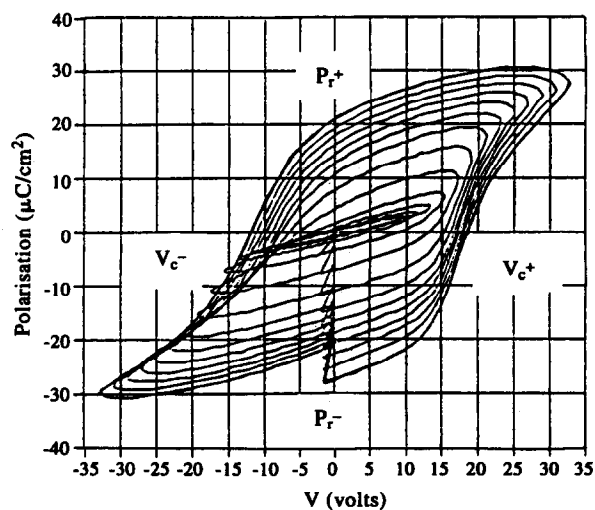


Fig. 7. Typical hysteresis loops with applied voltage between 10 and 30 V.

polarization is $P_r^+ = 18 \mu\text{C cm}^{-2}$ and $P_r^- = -22 \mu\text{C cm}^{-2}$ (at 30 V). The presence of leakage currents was observed at high voltages. It was found that at higher applied electric field strengths ($> 180 \text{ kV cm}^{-1}$) the layer became conducting. The relatively high coercive field compared to that of bulk ceramic may be associated with the fine grain microstructure of the film (150 nm). The stress stored in the film also influenced the high value of the coercive field. For an applied voltage below 15 V, the remanent polarization is equal to zero (Fig. 8); this proves the existence of a blocking layer between the ferroelectric material and the electrodes.

As we can observe on Fig. 7, the hysteresis loop showed a pronounced shift along the axis of the electric field. The asymmetry of the hysteresis loop for an unannealed top electrode sample is presented in Fig. 9 (low values of V_c^- compared to V_c^+); the saturation of the material is attained for a high applied voltage. The shift may be attributed to the existence of an internal field induced by the space charge effect (blocking layer) at the electrodes (top and bottom) and the PbTiO₃ layer interface (and may be at the grain boundaries and domain walls). The asymmetry tends to disappear when the top electrodes are annealed (450°C, 1 h). We must now optimize this annealing treatment. The possible interdiffusion at the interface of species such as Pb and Si and the for-

mation of a dielectric layer (we have observed, essentially on Si/SiO₂ substrates, the formation of lead silicate) with electrical properties different to the PbTiO₃ layer also affects the ferroelectric properties of the structure.

4 Conclusions

PbTiO₃ thin films were grown on silicon and platinized silicon substrates by RF magnetron sputtering. The growth conditions, thicknesses and annealing of the bottom Ti/Pt electrodes were optimized. PbTiO₃ films in these electrodes yielded films without holes or hillocks, with good adhesion and no electrical shorts in the test capacitors.

The presence of platinum has an important effect on the structure and microstructure of the PbTiO₃ films. The annealing treatment of the PbTiO₃ films was optimized, as well as on Si/SiO₂ and on Si/SiO₂/Ti/Pt substrates. The ferroelectric properties of the PbTiO₃ films were tested; it appears that annealing of the top electrode (Pt) plays a key role in the film properties. Without annealing, the hysteresis loop presents an important asymmetry (presence of an internal field) which is limited when an annealing treatment is performed. We must now optimize the top contact annealing and study whether the asymmetry of the loop is only due to a contact problem. The diffusion of lead must also perturb the electrical properties of the films.

Acknowledgements

The authors would like to thank P. Gaucher from Thomson LCR for help with electrical characterizations.

References

1. Budd, K. D., Dey, S. K. & Payne, D. A., *Br. Ceram. Proc.*, **36** (1985) 107.
2. de Keijser, M., Dormans, G. J. M., Van Veldhoven, P. J. & Larsen, P. K., *Integrated Ferroelectrics*, **3** (1993) 131.
3. Auciello, O., Mantese, L., Duarte, J., Chen, X., Rou, S. H., Kingon, A. I., Schreiner, A. F. & Krauss, A. R., *J. Appl. Phys.*, **73** (1993) 5197.
4. Wasa, K. & Hayakawa, S., *Thin Solid Films*, **52** (1978) 31.
5. Li, X., Liu, J., Zeng, Y. & Liang, J., *Appl. Phys. Lett.*, **67** (1993) 2345.
6. Kawaguchi, K., Adachi, H., Setsune, K., Yamazaki, D. & Wasa, K., *Appl. Opt.*, **23** (1984) 2187.
7. R miens, D., Jaber, B., Tirlet, J. F., Joire, H., Thierry, B. & Moriametz, Cl., *J. Eur. Ceram. Soc.*, **13** (1994) 493.
8. R miens, D., Jaber, B. & Jouan, P. Y., *J. de Physique IV*, **4** (1994) C2-107.
9. Azoulay, R., R miens, D., M nigaux, L. & Dugrand, L., *Appl. Phys. Lett.* **54**(19) (1989) 1857.

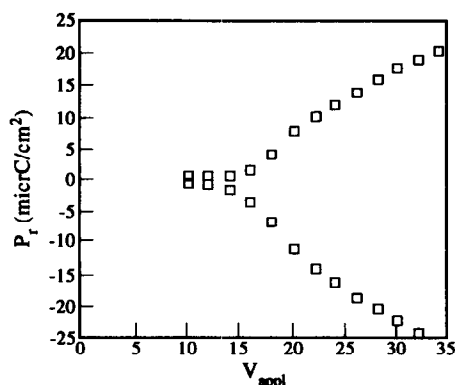


Fig. 8. Remanent polarization as function of applied voltage.

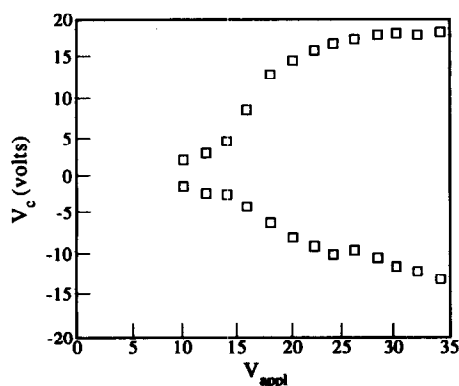


Fig. 9. Coercive voltage as function of applied voltage.